Scientific Research

Analysis of the High-Speed Impact Effect of Raindrops on Prestressed Wind Turbine Blades and the Equivalent Load Construction Method

Xiufeng Xu, Yichao Xu, Aiguo Zhou* and Zhengzhao Lai

Department of Mechatronic Engineering, Tongji University, Shanghai 200092, China
* Correspondence: zhouaiguo@tongji.edu.cn

Abstract: The finite element method and smoothed particle hydrodynamics (SPH) method are used to simulate the high-speed impact of a single raindrop on a prestressed wind turbine blade, and the factors affecting impact pressure and stress in a single raindrop impact, such as impact speed and raindrop diameter, are analyzed. In addition, the coupling generated by the simultaneous high-speed impact of dual raindrops is analyzed, and the effect of the distance between raindrop centers is analyzed. To address the difficulty in calculation due to the large number of impacting raindrops during the rainfall process, based on the calculation results of single raindrop impacts, the method of applying equivalent loads of raindrop impacts is proposed and validated by the stress distribution and the stress at each time point, thus ensuring the simulation accuracy of using the equivalent load of raindrop impact for the actual raindrop impact.

Keywords: prestressed wind turbine blade; raindrop impact; smoothed particle hydrodynamics

Citation: Xu, X.; Xu, Y.; Zhou, A.; Lai, Z. Analysis of the High-Speed Impact Effect of Raindrops on Prestressed Wind Turbine Blades and the Equivalent Load Construction Method. *Prestress Technology* **2024**, *2*, 01-18. https://doi.org/10.59238/j.pt.2024.02.001

Received: 29/05/2024
Accepted: 06/06/2024
Published: 30/06/2024

Publisher's Note: Prestress technology stays neutral with regard to jurisdictional claims in published maps and institutional affiliations.

1 Introduction

To meet the continuously growing global demand for energy, clean and renewable energy is needed. Compared with green energy sources such as solar and nuclear energy, wind energy has the advantages of large resource reserves, wide distribution, and high conversion efficiency suitable for large-scale industrial development. Wind is an indispensable clean energy source with an important strategic position in the energy structure, and it is one of the most promising renewable energy sources [1].

China is rich in wind energy resources. According to relevant statistics from the China Meteorological Administration, the exploitable capacity ranges from approximately 700 GW to 1.2 TW [2]. In China, wind energy resources are mainly distributed in inland areas such as North, Northeast and Northwest China, as well as in southeastern coastal areas and their surrounding islands [3].

Wind turbines are often installed on land. With the maturity of wind power technology, the number of offshore wind turbines is gradually increasing. In offshore wind farms, wind resources are rich and wind speed stability is high, so they can achieve higher stand-alone power generation while maintaining stable energy conversion efficiency. However, offshore wind farms experience abundant rainfall and are vulnerable to extreme weather conditions such as typhoons and heavy rains. Due to this harsh environment, the blades of offshore wind turbines are subjected to salt spray corrosion and the impact of raindrops, hail and other objects; thus, blade surface erosion can easily occur under this long-term action, seriously affecting the service life of prestressed blades. Due to higher rotation speeds and thinner wall

thicknesses, the prestressed blade tip region typically suffers the most severe rain erosion damage.

With the continuous development and maturity of wind power technology, to improve power generation efficiency and the ability to capture wind energy, wind turbine blades are becoming increasingly large, and their diameter is constantly increasing. An increase in the blade length continuously increases the maximum linear speed of the tip. Taking the 15 MW offshore wind turbine developed by Siemens Gamesa and General Electric as an example, the tip speed can exceed 100 m/s. The continuous increase in the linear speed of the blade tip increases the frequency and severity of rain erosion at the blade leading edge [4].

Wind power generation is mainly caused by the rotation of wind turbine blades driven by flowing air to convert wind energy into electricity. The blade is one of the core components of wind power equipment. Rain erosion damage causes the coating at the blade leading edge to fail, the surface roughness to gradually increase, and the blade shape to change. In the initial state of rain erosion damage, small pits with irregular distributions are generated on the pressure side of the wind turbine blade and in the area near the stagnation point; as damage accumulates, the pits connect with each other and develop into gouges. Long-term rain erosion causes the complete removal of the coating on the blade surface; this exposes the laminated plate under the coating, and delamination cracks can occur at the connection of the blade leading edge, which seriously affects the structural stability and dynamic performance of the prestressed blades and threatens production safety (Figure 1).

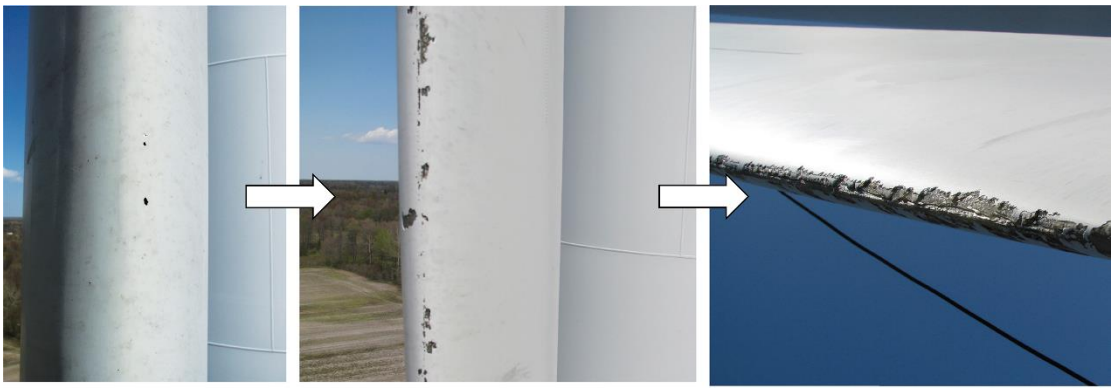

Figure 1 Changes in blade erosion [5]

The methods used to calculate raindrop impact include the impact method and the energy method. In the impact method, the water hammer equation or the computational fluid dynamics (CFD) are used to calculate the impact pressure of raindrops, and the finite element method is used to construct a wind turbine blade model to analyze the stresses generated by raindrop impact. Based on the principle of energy conservation, the energy method can better integrate the impact process with the mechanical characteristics of the impacting object; however, it is difficult to quantify the energy transfer between the rainfall field and wind turbine blades in actual calculations.

There have been many studies on blade leading edge erosion in China and abroad, but the focus has been on the effect of sand and gravel wear on blade leading edge erosion; there are fewer studies on leading edge blade erosion caused by raindrops. The calculations of raindrop impact have mainly focused on the stress generated by the single impact of a single or a small number of raindrops, and the

 https://doi.org/10.59238/j.pt.2024.02.001

erosion caused by the multiple impacts of multiple raindrops has been mainly obtained through experiments. However, rain erosion tests are costly and time-consuming. Reducing the cost of testing by simulating the impact of multiple raindrops remains an open issue.

2 Analyzing the High-Speed Impact Process of Raindrops on Prestressed Wind Turbine Blades

Due to the high linear speed at the tip of a large wind turbine blade, the leading edge is impacted by raindrops at high speeds during the sweeping process, resulting in severe rain erosion. A simulation of a single raindrop impact event on a wind turbine blade is performed to analyze the rain erosion damage generation process. The impact of high-speed raindrops on prestressed wind turbine blades is a solid–fluid coupling process, and the deformation and breakage of raindrops caused by the impact is a large deformation problem. Based on the consideration of calculation accuracy and time, the smoothed particle hydrodynamics (SPH) method is chosen for modeling and simulation, with the raindrop distribution in the natural environment as the basis.

2.1 Construction of a Model of Raindrops Impacting Wind Turbine Blades

2.1.1 Raindrop Physical Model

A simulation analysis of the high-speed impact of spherical raindrops is performed, and a model is constructed via the SPH method. The physical properties of water droplets can be defined by the Gruneisen equation of state [6]. The Gruneisen equation (see Formula (1)) relates the volume of liquid at a given temperature to the pressure to determine the pressure generated by the impact of compressible liquid:

$$P = \frac{\rho C^2 \mu \left[1 + \left(1 - \frac{\gamma_0}{2}\right)\mu - \frac{\alpha}{2}\mu^2\right]}{1 - (S_1 - 1)\mu - S_2 \frac{\mu^2}{\mu + 1} - S_3 \frac{\mu^3}{(\mu + 1)^2}} + (\gamma_0 + \alpha\mu)e \tag{1}$$

where C is the speed of sound in the liquid, S_1, S_2, and S_3 are the fitting coefficients, γ_0 is the Gruneisen coefficient, α is the first-order volume modification, ρ is the density of the liquid, μ is the dynamic viscosity of the liquid, and e is the internal energy per unit volume.

The parameters of the raindrop physical material model are shown in Table 1.

Table 1 Parameters for the raindrop physical material model [6]

$\boldsymbol{\rho}$ $\left(\mathbf{kg/m^3}\right)$	$\mathbf{v_s}$ $(\mathbf{Pa \cdot s})$	$\mathbf{C}$ $(\mathbf{m/s})$	$\boldsymbol{\alpha}$	$\mathbf{S_1}$	$\mathbf{S_2}$	$\mathbf{S_3}$
1000	0.001	1480	0	2.56	-1.986	0.226

2.1.2 Structure and Material Properties of the Prestressed Blade Panels

The structure of a prestressed wind power blade mainly includes the blade tip, blade root, blade leading edge, blade trailing edge, and internal supporting main beam and shear web; the cross-sectional structure is shown in Figure 2a) [7]. According to the parameter information for a Sandia all-glass baseline wind turbine blade, the composite panel structure is composed of a bottom composite layer, a middle foam layer, an upper composite layer, and a surface coating, as shown in Figure 2b). The thicknesses of the upper and bottom composite layers are both 5 mm, and the material used is a QQ1 composite material consisting of Vantico TDT 177-155 epoxy resin, Saertex U14EU920-00940-T1300-100000 0 fiber and VU-90079-00830-01270-000000 45 fiber. The thickness of the middle layer is 5 mm, and the material used is

Corecell™ M-Foam M200. The coating thickness is 0.6 mm, and the material used is epoxy resin [8].

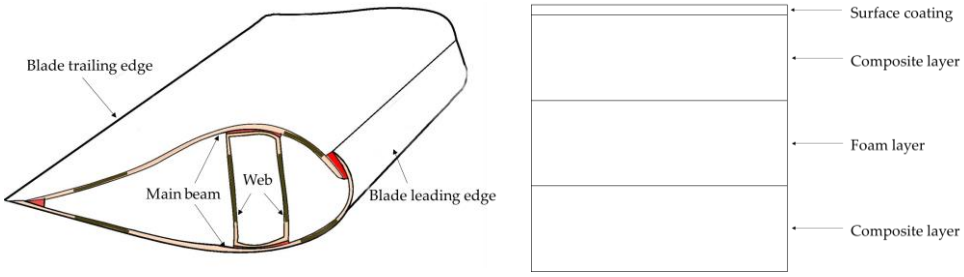

a) Blade cross-section structure [7] b) Panel structure composition

Figure 2 Blade cross-section structure and panel composition

Table 2 lists the material properties of each layer of the prestressed wind turbine blade panel.

Table 2 Material properties of each blade layers [8]

Material properties \ Material type		Coating	Foam layer	QQ1
Density	ρ $(kg \cdot m^{-3})$	1235	200	1919
Longitudinal Young's modulus	E_1 (GPa)	3.44	0.256	33.10
Transverse Young's modulus	E_2 (GPa)	3.44	0.256	17.10
Shear modulus	G_{12} (GPa)	1.38	0.098	6.29
Poisson's ratio	v_{12}	0.30	0.330	0.27

2.2 SPH Method-Based Analysis of the High-Speed Impact of a Single Raindrop on a Blade

In a natural rainfall field environment, the speed and size distribution of raindrops are random, and the impact process between the leading edge of the wind turbine blade and the raindrops is similar and repeatable. Therefore, by simulating the impact process of a single raindrop and the leading edge of wind turbine blades by the SPH method, the effect of raindrops impacting the blades during natural rainfall is analyzed.

To ensure that the whole influence area of a single raindrop impact process is included and to improve the simulation accuracy while saving computational resources, since the influence area of raindrop impact is usually a circle at 10 times the raindrop diameter, a blade panel model of 25×25×15.6 mm is constructed. The bottom and sides of the panel model are completely fixed, and the size of the coating mesh in the model is refined. In the center of the constructed blade panel model, a raindrop with a diameter of 2 mm tangent to the panel is placed, and its initial speed is set to 90 m/s. After the mesh is generated, the raindrop is converted to an SPH particle, and the contact process within 50 μs of a single raindrop impacting vertically on a blade is simulated by the SPH method.

The raindrop SPH particle speed during the impact process is analyzed. The raindrop SPH particle speed contours at the central cross-section at each moment are

 https://doi.org/10.59238/j.pt.2024.02.001

shown in Figure 3. To better represent the speed distribution and variation in raindrop particles, the upper limit of the speed is 250 m/s, i.e., the red area in the diagram, and 0 mm/s is used as the lower limit, i.e., the blue area in the diagram.

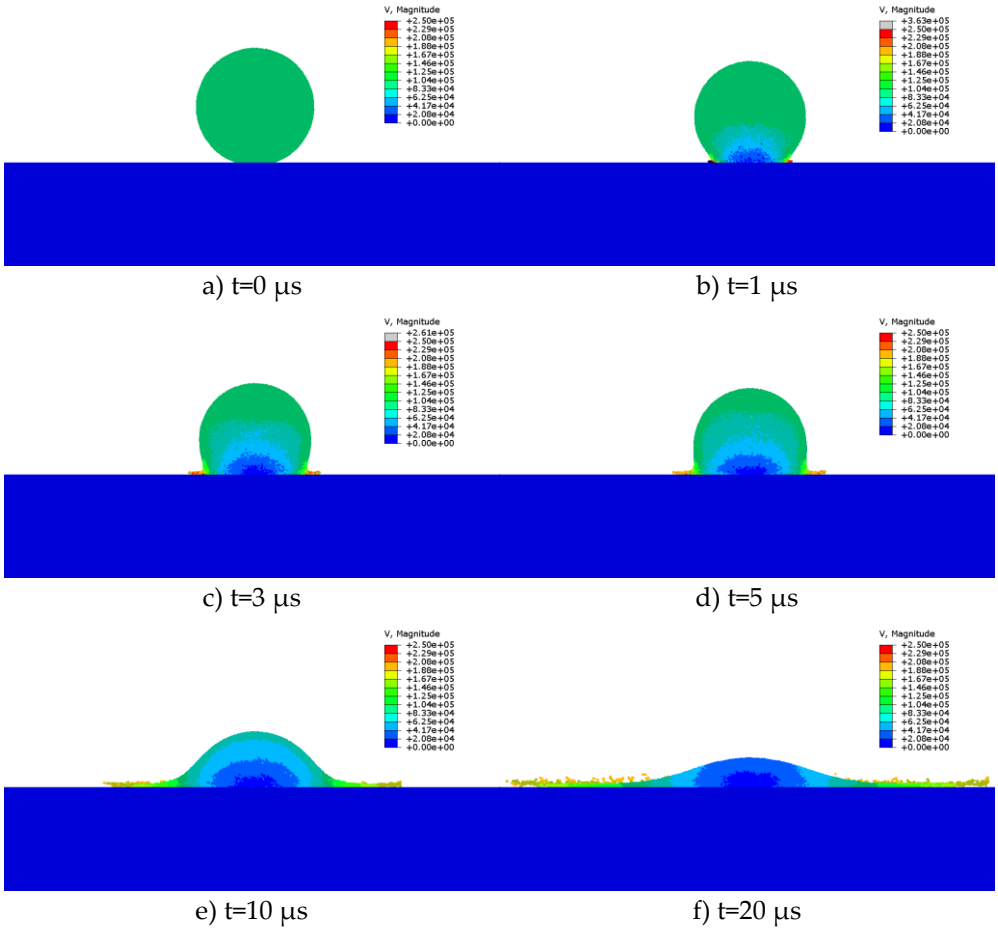

Figure 3 Raindrop speed at central cross-section

During the impact process, the particle speed at the contact edge between the raindrop and the blade coating first increases and then decreases. The raindrop is initially in a compressed state; part of it first contacts with the coating and is located in the center, and particle speed decreases rapidly; part of it contacts the edge, the particle velocity increases rapidly, and it ejects along the surface of the coating. At this time, most of the particles maintain speed, the raindrop maintains an overall spherical state, and the raindrop impact contacting edge part of the coating surface forms a lateral jet. The lateral jet reaches a maximum speed of 363 m/s at 1 μs (Figure 3b)), then decreases rapidly and remains at approximately 200 m/s, as shown in Figure 3c) and Figure 3d). As the impact process proceeds, the liquid breaks through the surface tension and spreads along the coating surface. At this time, the speed of most particles in the raindrop center gradually decreases to approximately 20 m/s, while the particles at the contact edge between the raindrops and the coating maintain their initial speed and are sprayed along the direction of the coating, while a part of the raindrop splashes, as shown in Figure 3e) and Figure 3f).

The impact pressure load generated on the prestressed wind turbine blade coating surface after impact by a 2 mm diameter raindrop at 90 m/s is analyzed, and the maximum impact pressure on the coating surface at each moment is extracted, as

shown in Figure 4. The maximum load generated at 0.6 μs after impact is 73.4 MPa, similar to the 76.6 MPa calculated by the water hammer equation, decreases rapidly to 10 MPa within 10 μs, and then decreases slowly.

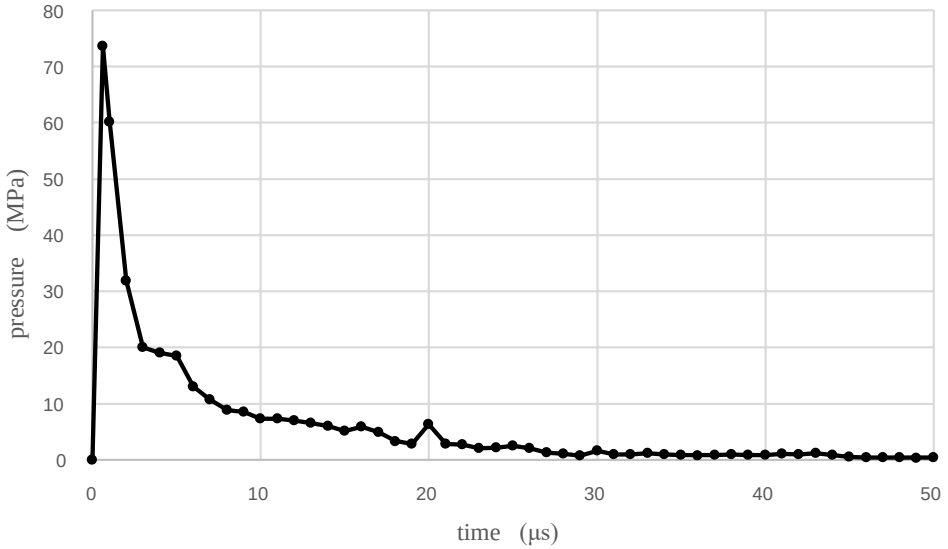

Figure 4 Impact pressure load–time curves on the coating surface

The equivalent von Mises stress contours on the upper surface of the blade coating and the cross-section of the impact center on the blade panel at different times after impact are extracted, as shown in Figure 5, where the stress distribution on the upper surface of the coating is on the left side and the stress distribution in the central cross-section is on the right. A display threshold of 1 MPa is used to display the stress wave more intuitively, and the portion above the threshold is shown in gray.

As shown in Figure 5, during the impact of high-speed raindrops on the blade coating, Rayleigh waves are generated and propagate from the impact contact center of raindrops and coatings to the free boundary of the blade model; at the same time, vertical and lateral body waves are generated, and there is interference between the waves. During the raindrop impact process, the stresses of contact area with the blade coating and the stress propagation area under the coating interface are relatively large. The high stress on the coating surface is generated by the peak pressure generated by the impact of raindrops, and the high stress under the interface is the superposition of the shock wave front and part of the stress generated by the local high pressure. The large stress distribution indicates that the microcracks due to the blade rain erosion may occur in the impact contact area between raindrops and blade coating and the area under the coating interface. Due to the different material properties of the different layers of the blade panel model, there is an obvious interface in the stress distribution. The constructed model is based on a perfect combination of different materials so that the deformation of the different materials between the layers is the same, while the Young's modulus of different materials is different, so the generated stresses are different.

During the initial contact stage of raindrop impact, the stress at the impact contact center increases rapidly to form a high-stress area, which is transmitted downward along the thickness of the blade panel. As the impact contact area between raindrops and blades increases, the stress at the impact center gradually decreases.

https://doi.org/10.59238/j.pt.2024.02.001

Due to the interference of stress waves and reflected waves, an annular high-stress region is generated at the impact contact edge.

The maximum strain of the coating material on the prestressed wind turbine blade at failure is 0.3ε [9]. During the impact process, the maximum plastic strain generated by the prestressed wind turbine blades is approximately 0.0055ε, which is far from the value that can cause damage. Therefore, rain erosion damage occurs after multiple impacts from raindrops.

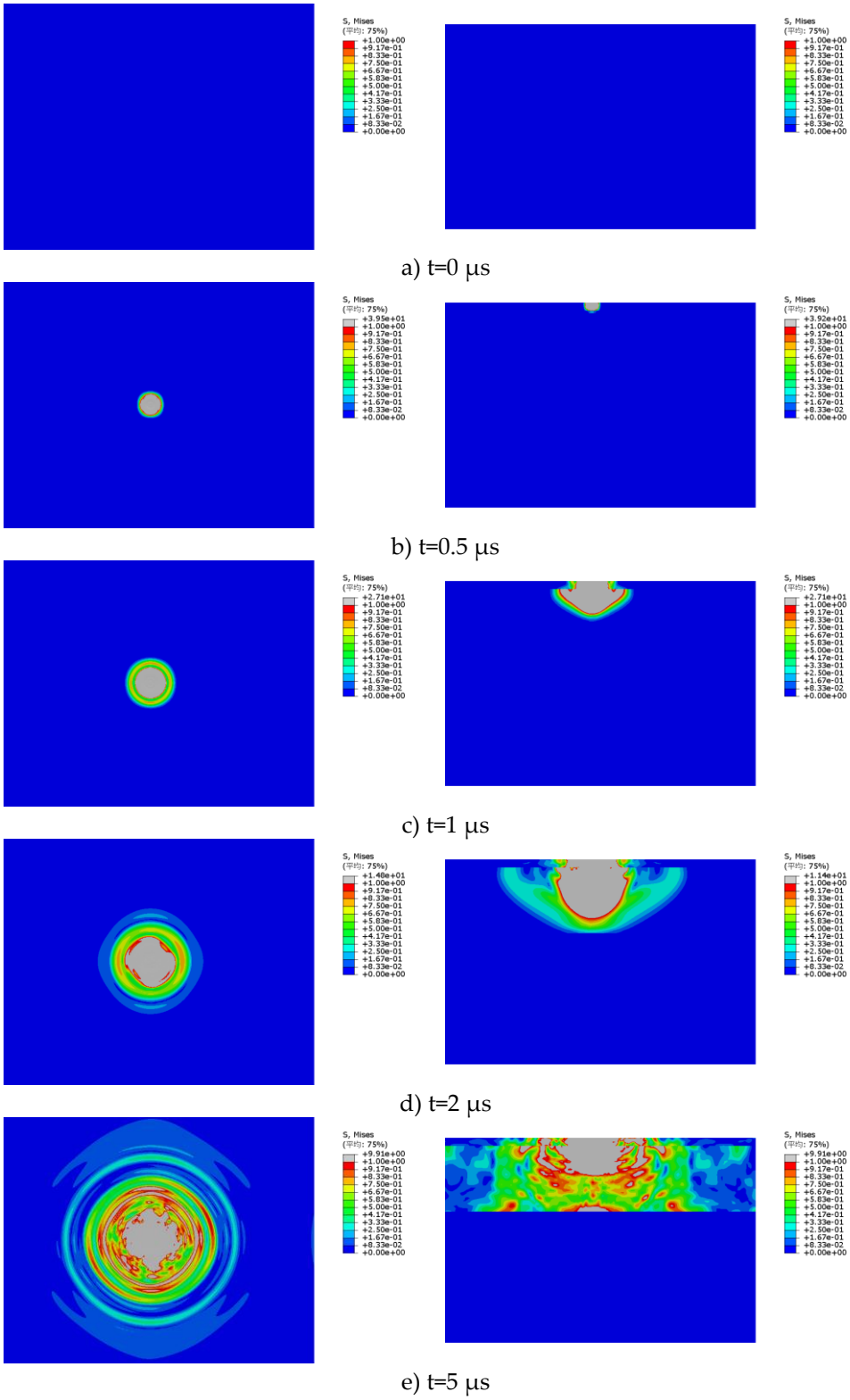

a) t=0 μs

b) t=0.5 μs

c) t=1 μs

d) t=2 μs

e) t=5 μs

Figure 5 Stress contours on the blade coating surface (left) and central cross=section (right)

3 Construction of an Equivalent Load of High-Speed Raindrop Impact on Prestressed Wind Turbine Blades

The rain erosion damage of the leading edge of the prestressed wind turbine blade is the accumulation of fatigue damage under the long-term impact of raindrops. The high-speed impact of a single raindrop cannot directly damage the prestressed wind turbine blades. However, during the generation and evolution of rain erosion damage, the number of raindrops is large; therefore, the single raindrop impact simulation cannot be used for many raindrops throughout the whole rain erosion process since the simulation time could be too long. The SPH method is used to analyze the pressure and stress factors affecting the single raindrop impact, and the equivalent load of raindrop impact, which is used for the accelerated calculation of impact of many raindrops in the rain erosion process, is constructed and validated. The simulation of dual high-speed raindrops impacting the blade at the same time is performed to verify whether the coupling effect on the impact of raindrops could be ignored and whether the impact of multiple raindrops during the rain erosion process could be accelerated by using the equivalent load of raindrop impact.

3.1 Raindrop Distribution

Raindrops can be considered to be uniformly distributed in the rainfall space, and the volume of the rainfall space V_f can be calculated by the following equation (2) [9]:

$$V_f = S \times V_{rain} \times t_{rain} \tag{2}$$

where S is the area of the rainfall projection area, t_{rain} is the rainfall duration, and V_{rain} is the raindrop speed.

The number of raindrops usually follows a Poisson distribution. The probability that the number of raindrops $N(V_f)$ in a unit volume V_f of rainfall space is equal to k, then the probability $P\left(N\left(V_f\right)=k\right)$ is [10]:

$$P\left(N\left(V_f\right)=k\right)=\frac{\left(\lambda_{rain}V_f\right)^k e^{-\lambda_{rain}V_f}}{k!} \tag{3}$$

where λ_{rain} is the expectation for the number of raindrops in the unit volume, which can be expressed by a power law function, see Formula (4) [11]:

$$\lambda_{rain} = 48.88I^{0.15} \tag{4}$$

where I is the rainfall intensity in mm/h.

In natural rainfall fields, large raindrops have difficulty maintaining large diameters under the influence of air resistance and are often broken into several small raindrops, and raindrops larger than 5 mm have a very small probability of occurring. The cumulative distribution of raindrop diameters is expressed by the following equation (5) [10]:

$$F = 1 - exp\left[-\left(\frac{d}{1.3I^{0.232}}\right)^{2.25}\right] \tag{5}$$

where d is the raindrop diameter in mm and I is the rainfall intensity.

Figure 6 shows the probability density curve and cumulative distribution curve of raindrop diameter for different rainfall intensities of 1 mm/h, 5 mm/h, 10 mm/h, 25 mm/h, and 50 mm/h.

 https://doi.org/10.59238/j.pt.2024.02.001

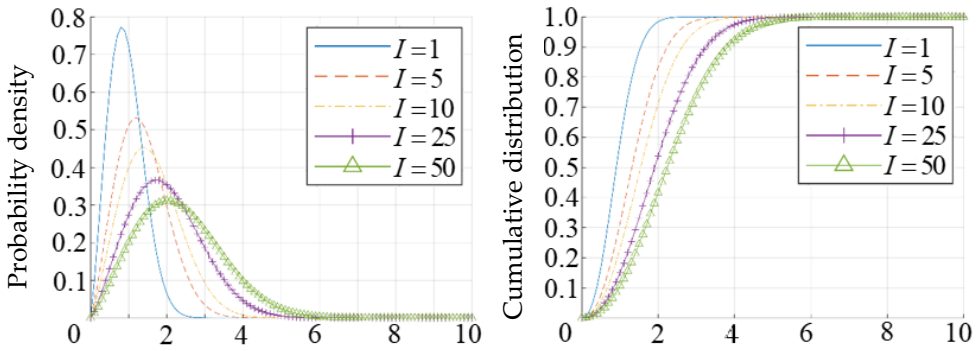

a) Raindrop diameter probability density curve

b) Raindrop diameter cumulative distribution curve

Figure 6 Distributions of raindrop diameters under different rainfall intensities

As shown in Figure 6, for rainfall intensities below 10 mm/h, the diameter of most raindrops is less than 3 mm, and for rainfall intensities below 50 mm/h, the diameter of most raindrops is less than 5 mm. The rainfall grades in China are divided according to two time periods: 24 h and 12 h, as shown in Table 3 [12]. A 12-hour rainfall greater than 140 mm or a 24-hour rainfall greater than 250 mm is a relatively rare extremely torrential rain, so most rainfall intensity is less than 10 mm/h. Therefore, in a natural rainfall field, the diameter of most raindrops is concentrated between 1 mm and 3 mm, and raindrops with a diameter greater than 3 mm can be ignored.

Table 3 Rainfall grades for different time periods [12]

Grade	Rainfall for different time periods (mm)	
	12 h	24 h
Trace rainfall (scattered light rain)	<0.1	<0.1
Light rain	0.1-4.9	0.1-9.9
Moderate rain	5.0-14.9	10.0-24.9
Heavy rain	15.0-29.9	25.0-49.9
Rainstorm	30.0-69.9	50.0-99.9
Torrential rain	70.0-139.9	100.0-249.9
Extremely torrential rain	≥140.0	≥250.0

3.2 Analysis of Influencing Factors of High-Speed Raindrop Impact Load Based on SPH Method

The natural rainfall environment is more complicated, so the impact speed of raindrops on blades and the effect of raindrop diameter on raindrop impact are analyzed.

In the natural environment, raindrops with a diameter of 2 mm have the highest distribution probability among intense rainfall events. Therefore, the time history of the impact pressure generated by the raindrops with a diameter of 2 mm at 70 m/s, 90 m/s, and 110 m/s impacting blades is shown in Figure 7. In addition to the speeds listed in the Figure 7, for speeds of 70 m/s to 110 m/s, the maximum impact pressure of raindrops is generated within 1 μs and rapidly decreases to 10 MPa within 10 μs and then decreases slowly, approaching 0 at approximately 30 μs.

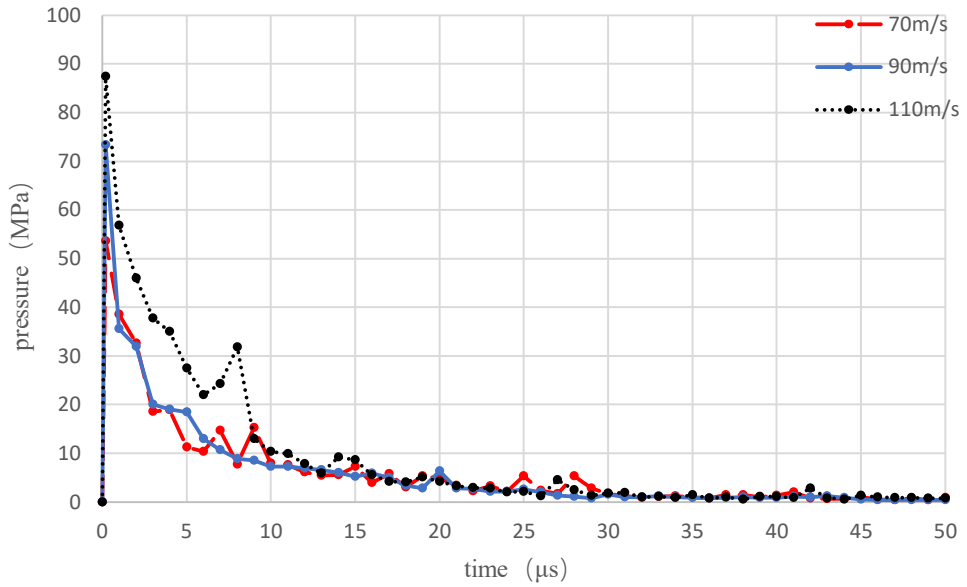

Figure 7 Impact pressure–time curves of 2 mm raindrops with different speeds

With 5 MPa as the lower limit, the pressure action area generated by the impact of 2 mm diameter raindrops on the coating surface of the wind turbine blades at different speeds is shown in Figure 8. The pressure action area generated by the impact of a 2 mm diameter raindrop on the blade at a speed of 70 m/s reaches a maximum value of 2.75 mm^2 at 7 μs and decreases to 0 at 16 μs; the pressure action area generated by the impact at a speed of 90 m/s reaches a maximum value of 3.77 mm^2 at 7 μs and decreases to 0 at 18 μs; and the pressure action area generated by the impact at a speed of 110 m/s reaches a maximum value of 4.66 mm^2 at 8 μs and decreases to 0 at 17 μs.

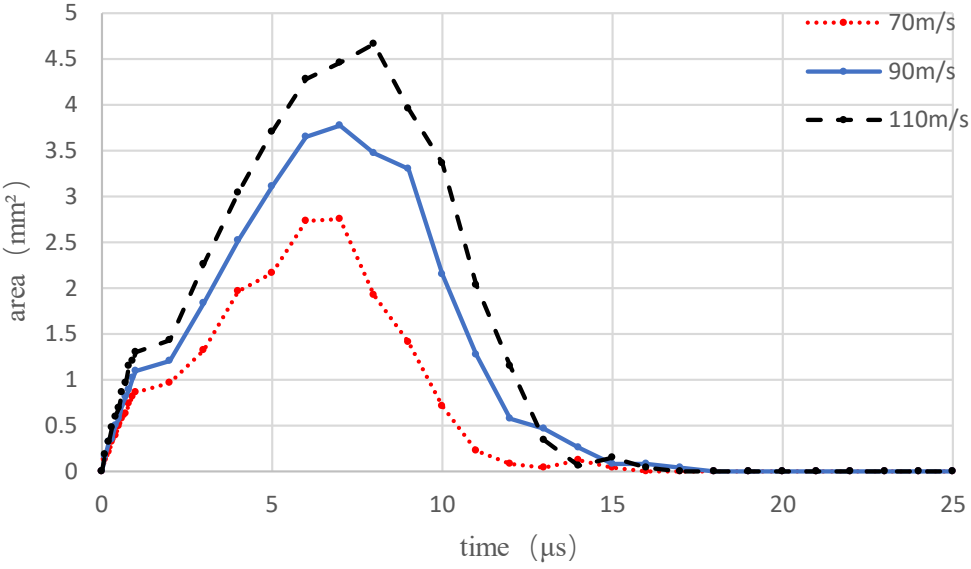

Figure 8 Area–time curves of impact pressure of 2 mm raindrops at different speeds

The time history of the maximum pressure generated by raindrops with diameters of 1 mm, 2 mm and 3 mm at a speed of 90 m/s on the wind turbine blades is shown in Figure 9. The maximum impact pressure by raindrops is generated within 1 μs, rapidly decreases to approximately 10 MPa within 10 μs, and then decreases slowly to approach zero at approximately 30 μs.

https://doi.org/10.59238/j.pt.2024.02.001

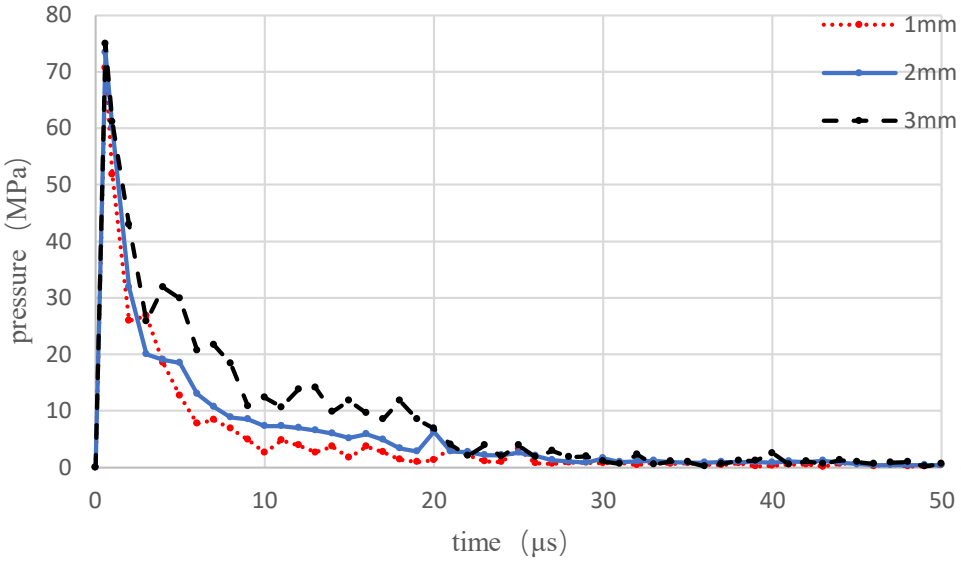

Figure 9 Impact pressure–time curves of raindrops with different diameters at 90 m/s

With 5 MPa as the lower limit, the pressure action area generated by raindrops with diameters of 1 mm, 2 mm, and 3 mm impacting the coating surface of the wind turbine blades at a speed of 90 m/s is shown in Figure 10. The impact pressure action area of raindrops with diameter of 1 mm reaches a maximum of 0.97 mm² at 4 μs and decreases to 0 at 9 μs. The impact pressure action area of raindrops with a diameter of 3 mm reaches a maximum value of 8.31 mm² in 10 μs and decreases to 0 at 21 μs.

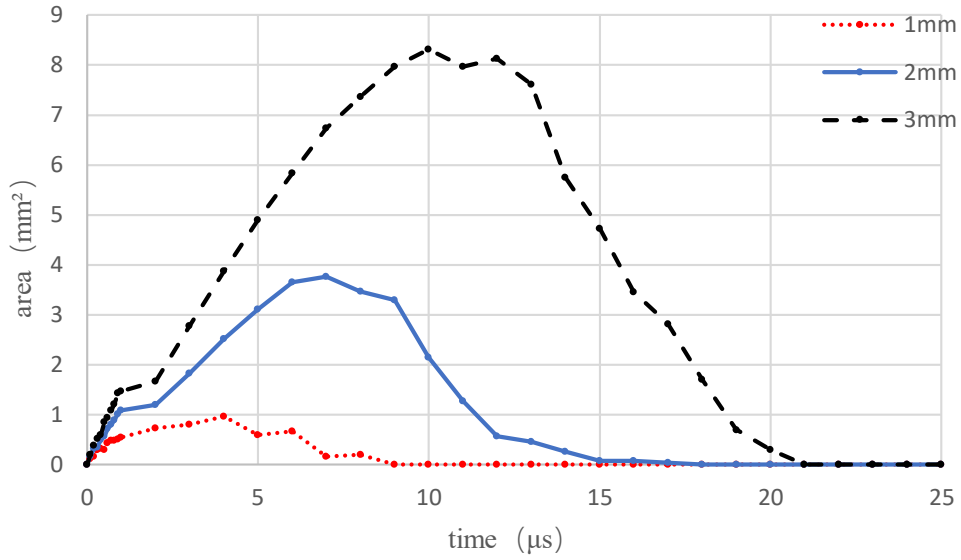

Figure 10 Area–time curves of impact pressure of raindrops with different diameters at 90 m/s

The analysis shows that the action area of raindrop impact pressure and the action time of impact pressure increase with increasing raindrop diameter and impact speed, but they are mainly affected by raindrop diameter rather than impact speed. The impact pressure action area is approximately equal to the maximum cross-sectional area of a raindrop.

3.3 Construction and Validation of the Equivalent Load of High-Speed Raindrop Impact

In the natural environment, the impact of a single raindrop or a small amount of raindrops cannot directly cause damage to the coating of a prestressed wind turbine blade, and the rain erosion of the wind turbine blade is the result of the long-term impact of high-speed raindrops. The SPH method-based simulation of a single raindrop impact on a wind turbine blade by a single computer (CPU processor: i7-

13700HX, memory: 32GB) could take nearly 2 hours, so it is difficult to perform simulation on the entire process of raindrop impact on a wind turbine blade.

To improve the simulation efficiency, an impact load is constructed based on the simulation of raindrop impact on a wind turbine blade. The load is applied to the raindrop impact area on the upper surface of the coating to ensure accuracy and increase the calculation speed.

The high-speed raindrop impact load is constructed based on the impact pressure and pressure action area. The simulation analysis of raindrops impacting wind turbine blades due to different factors reveals that impact pressure is mainly determined by raindrop impact speed and can be quickly calculated by the water hammer equation, while the pressure action area is mainly determined by raindrop diameter. The impact pressures and pressure action areas under different raindrop impact loads are obtained through the simulation of a single raindrop impact. Taking a raindrop with a diameter of 2 mm impacting a wind turbine blade at 90 m/s as an example, a load model is constructed based on the simulation results using the SPH method, and the pressure and action area at each moment are shown in Figure 11.

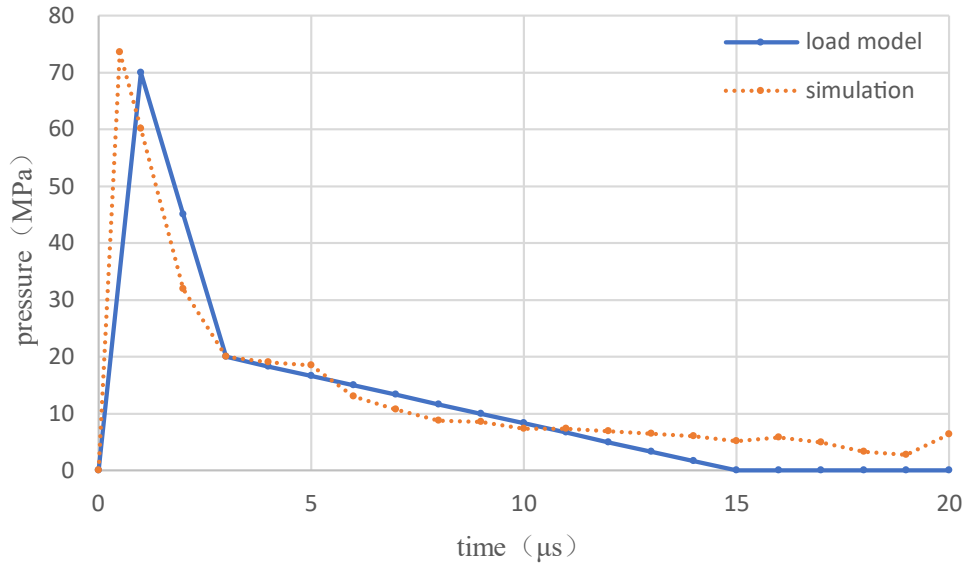

a) pressure

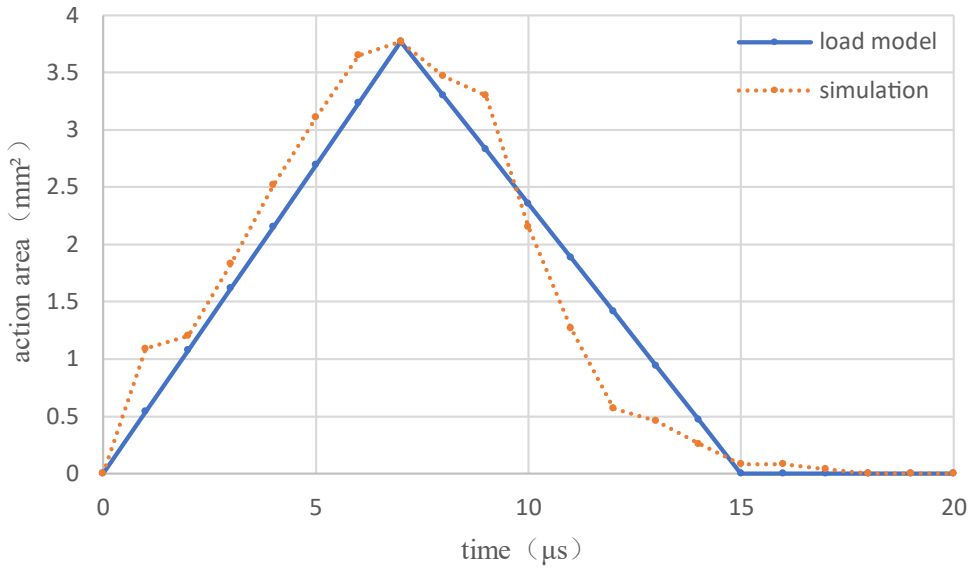

b) action area

Figure 11 Pressure and action area calculated by load model and simulation

https://doi.org/10.59238/j.pt.2024.02.001

Simulation of the constructed load applied to the prestressed wind turbine blade coating shows that the stress reaches a maximum at 1 μs. To make the results more intuitive, the stress contours of the central cross-section when the output stress reaches the maximum value with 1 MPa as the upper limit are compared with the simulation results of raindrop impact using the SPH method, as shown in Figure 12. The simulation results of the applied load are on the left, the simulation results of raindrop impact by the SPH method are on the right, and the stress distributions of the central cross-sections are similar when the stress is maximum.

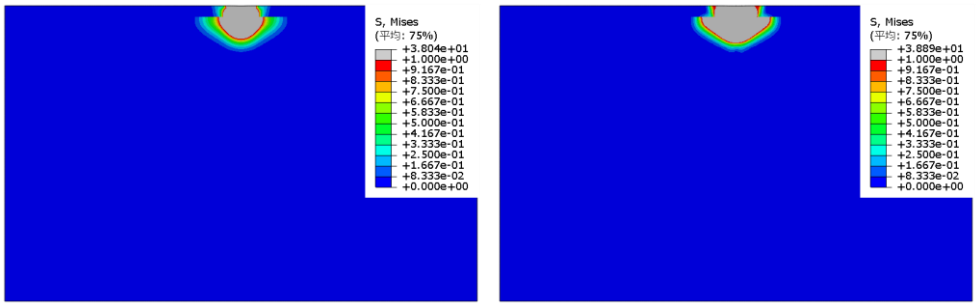

a) Load model b) Raindrop impact

Figure 12 Comparison of stress contours

The stress–time curves of the applied load model simulation and the raindrop impact simulation are shown in Figure 13.

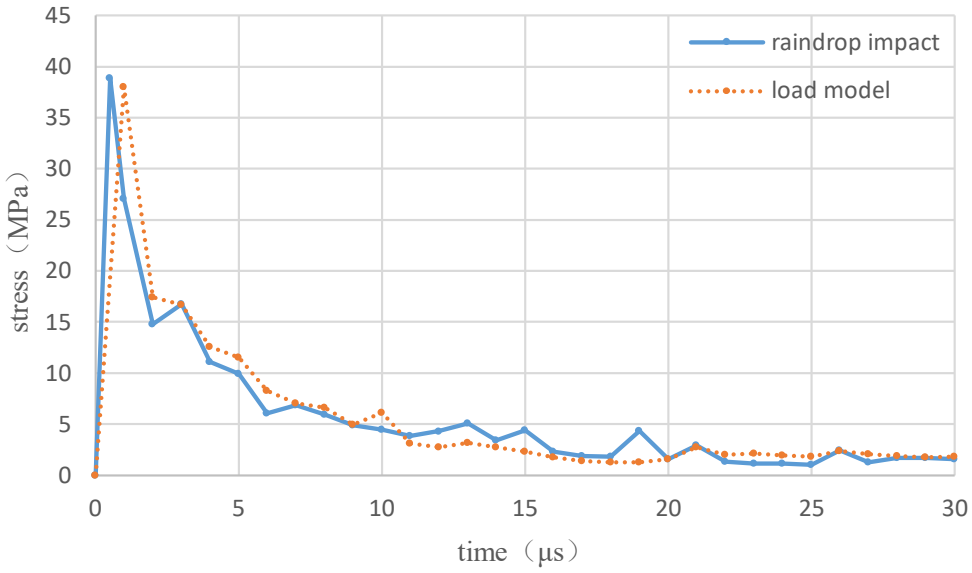

Figure 13 Comparison of stress–time curves

During the impact of raindrops, the pressure on the coating surface reaches a maximum at 0.5 μs, while the load model simulation reaches a maximum pressure at 1 μs; therefore, there is some difference in the time required for the two to reach the maximum stress, and for other moments, the difference is relatively small.

The simulated stress distribution and the stress at each time point are similar for the two simulations of applying the constructed load on the upper surface of the coating and the raindrop impacting coating. Therefore, the approximate calculation of raindrop impact can be performed by constructing a load model.

3.4 Load Analysis of the Dual Raindrop Coupling Impact Based on the SPH Method

If the rainfall intensity in the natural rainfall environment is strong and raindrops are densely distributed in the air, multiple raindrops are prone to multiple

impacts and collisions with a small area of prestressed wind turbine blades in a relatively short time, resulting in raindrop coupling. In the natural rainfall field, the time interval between two consecutive raindrop impacts on the same point on the prestressed wind turbine blade is three orders of magnitude longer than the duration of the stress wave generated by the impact of a single raindrop. On the other hand, the probability of the occurrence of three or more raindrops impacting on a small area of the prestressed wind turbine blade without interference is small and could be ignored [13]. Therefore, only the effect of the distance interval on raindrop coupling when the prestressed wind turbine blade is impacted by double raindrops is analyzed, and the effect of the time interval on raindrop coupling is ignored.

Figure 14 shows the speed contour in the vertical direction (i.e., the impact direction) at each time point in the SPH simulation results of the coupling impact of dual raindrops with a spacing of 3 mm and a diameter of 2 mm. To make the results more intuitive, the initial speed direction of raindrops is the negative direction, and the upper and lower speed limits are set to 200 m/s and -90 m/s, respectively. The pair of raindrops with a spacing of 3 mm starts to couple when they impact each other at 5 μs. Under the coupling effect, the raindrop particles in the central contact part splash in the direction away from the prestressed wind turbine blades, but the number of particles affected by the coupling only account for a small part, and the coupling effect is limited.

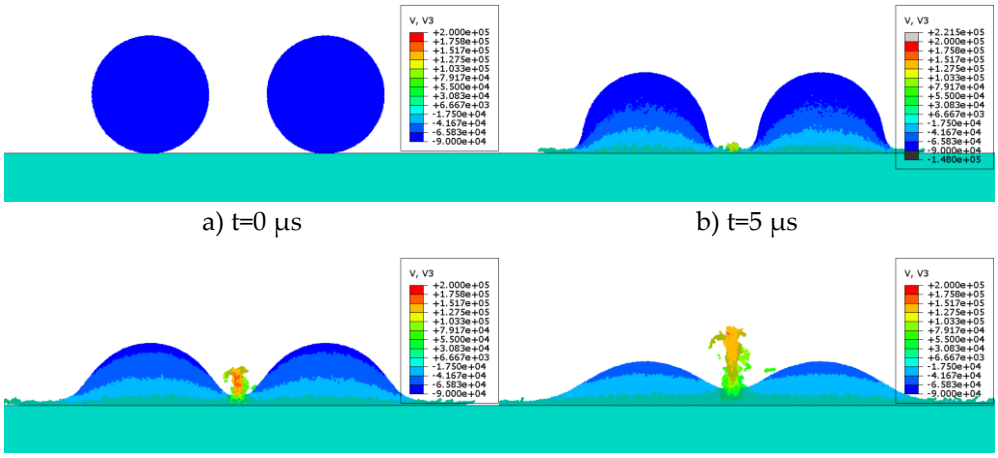

a) t=0 μs b) t=5 μs

c) t=10 μs d) t=15 μs

Figure 14 Impact speed of double raindrops with 3 mm spacing along the vertical direction

When the coupling of double raindrops with a distance of 3 mm or 5 mm is generated, in addition to the area in direct contact with the coating of prestressed wind turbine blade, the central area of the double raindrop spacing is subjected to the impact pressure generated by the splashing liquid particles, as shown in Figure 15. There is no such pressure area on the coating surface when the distance of double raindrops is 8 mm and 10 mm.

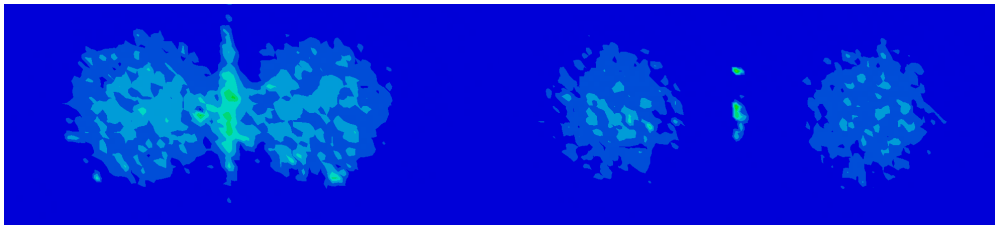

a) Double raindrops with 3 mm spacing b) Double raindrops with 5 mm spacing

Figure 15 Impact pressure of double raindrops impacting the coating surface

With 5 MPa as the lower pressure limit, the impact pressure area–time curves generated by the impact of double raindrops under different spacings are shown in

https://doi.org/10.59238/j.pt.2024.02.001

Figure 16. Under the coupling action of double raindrops with spacings of 3 mm and 5 mm, the maximum impact pressure action areas on the coating surface are 7.86 mm^2 and 7.69 mm^2, respectively; compared to the maximum impact pressure action area generated by the impact of double raindrops with no coupling, which is 7.54 mm^2, the area is increased by 1.04 and 1.02 times, respectively. Therefore, raindrop coupling has a limited effect on the impact pressure action area.

The time curves of impact pressure generated by the impact of a single raindrop and double raindrops with different spacing distances are shown in Figure 17.

The maximum pressures generated by the impact of double raindrops with a diameter of 2 mm and a distance of 3 mm, 5 mm, 8 mm and 10 mm are 77.69 MPa, 77.39 MPa, 77.22 MPa and 77.19 MPa, respectively, which are all approximately the maximum pressures generated by the impact of a single 2 mm diameter raindrop (73.6 MPa). The rate of decrease in the impact pressure under dual raindrop coupling is 1.05 times lower than that under single raindrop impact, but the speed change is smaller. Therefore, the effect of the coupling of dual raindrops with different spacings on the generated impact pressure is limited.

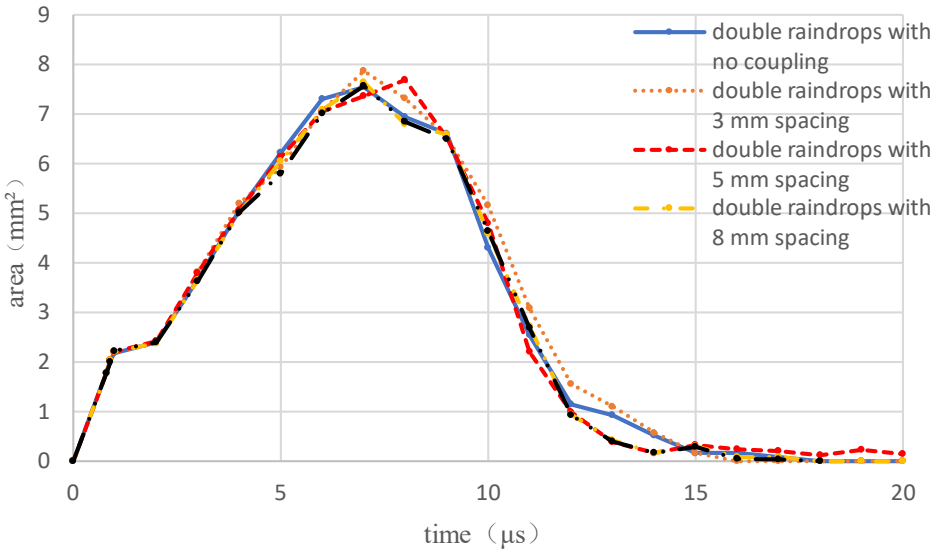

Figure 16 Impact pressure area–time curves of the coupling of dual raindrops impacting on the coating surface

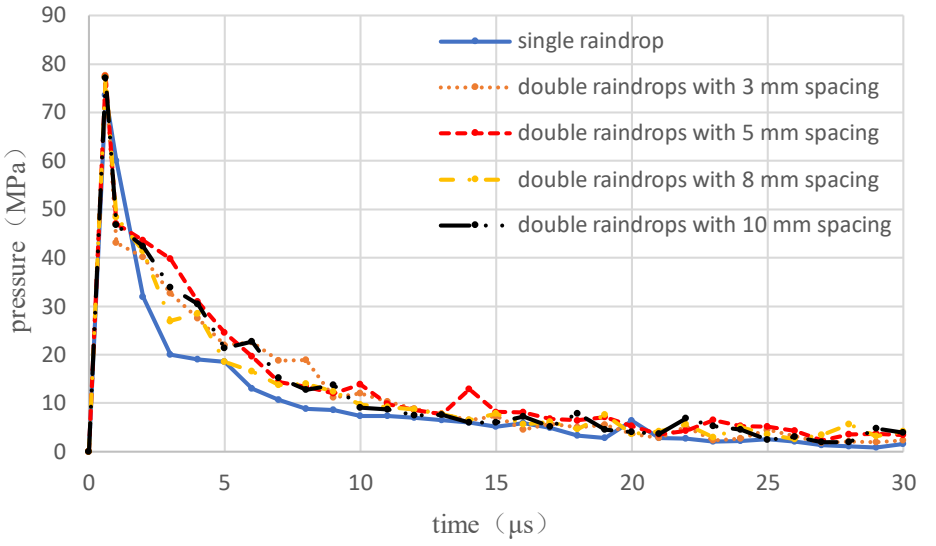

Figure 17 Pressure–time curves for single raindrop and double raindrop coupling

The impact stress–time curves of a single raindrop and double raindrops with different spacings are shown in Figure 18. The maximum stresses generated by the impact of dual raindrops with a diameter of 2 mm and a distance of 3 mm, 5 mm, 8 mm and 10 mm are 39.83 MPa, 39.81 MPa, 39.82 MPa and 39.83 MPa, respectively, which are almost the same as the maximum stress generated by the impact of a single 2 mm diameter raindrop (38.89 MPa). Compared to the maximum stress at each time point caused by the impact of a single raindrop, under dual raindrop coupling, the stress at each time point (except the maximum stress generated by the initial impact contact) shows a second stress peak at 10 μs and 11 μs, which arises from the interference between the stress waves generated by the impact of different raindrops, rather than from the coupling between two raindrops.

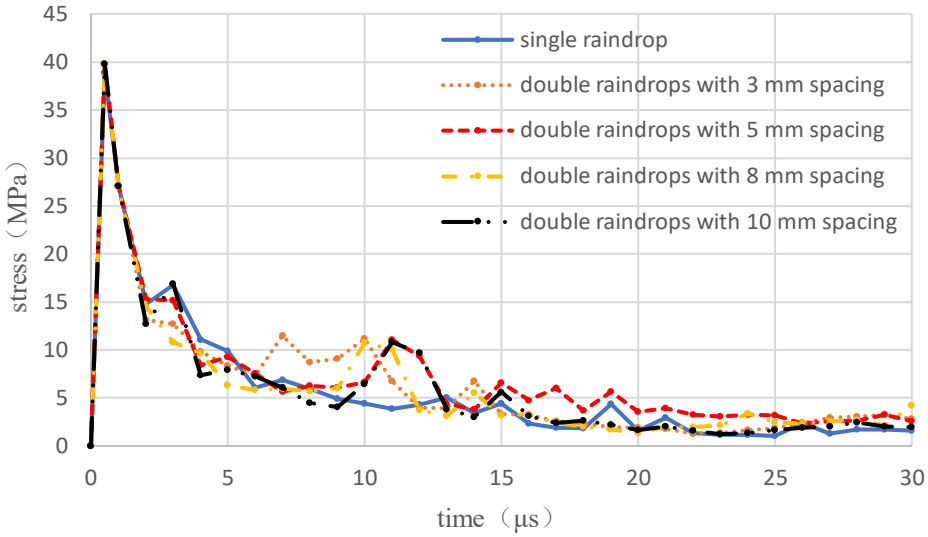

Figure 18 Stress–time curves of single raindrop and double raindrop coupling

Based on comprehensive consideration of the impact pressure, impact pressure area and impact stress generated in the simulation results of single raindrop impact and double raindrop coupling using the SPH method, in the process of multiple raindrop impact on prestressed wind turbine blade, the pressure and stress generated by double raindrops impacted at the same time with a certain distance are only slightly different from those of the single raindrop impact, and other coupling cases of multiple raindrop impact (> 2 raindrops) are negligible, so the rain erosion of prestressed wind turbine blades produced in the natural environment can be regarded as the cumulative result of fatigue damage produced by the load generated by a single raindrop impact repeated many times on the surface of prestressed blades, and the simulation of raindrop impact in the rain erosion damage evolution process of prestressed wind turbine blades can be accelerated by using the equivalent load of raindrop impact.

4 Conclusions

This paper proposes an accelerated calculation method for simulating the multiple impacts of raindrops in terms of rain erosion by applying the impact load of an equivalent raindrop based on the simulation results of a single raindrop impact. Using the SPH method, the simulation of raindrops with a diameter ranging from 1 to 3 mm impacting a prestressed wind turbine blade at a high-speed ranging from 70 to 110 m/s is performed. The maximum impact pressure generated by a single raindrop impact is determined by the raindrop impact speed and can be approximated by the water hammer equation. The impact pressure action area is determined by the raindrop diameter. The SPH method is used to simulate the coupling impact of double raindrops with a center spacing of 3 to 10 mm and a diameter of 2 mm at 90 m/s.

https://doi.org/10.59238/j.pt.2024.02.001

The coupling has a limited effect on the impact pressure, impact stress, and impact pressure action area at each time point. The analysis of the factors influencing the impact pressure of single raindrop and double raindrops provides the basis for the construction of a model using the equivalent load of raindrop impact. Based on the simulation results of single raindrop impact, a model using the equivalent load of raindrop impact is constructed and validated through stress distribution and stress values at different times. On the premise of ensuring calculation accuracy, the model using the equivalent load of raindrop impact provides an effective method for accelerating the simulation of prestressed wind turbine blades under the multiple impacts of raindrops.

Conflict of Interest: All authors disclosed no relevant relationships.

Date Availability Statement: The data that support the findings of this study are available from the corresponding author, Zhou, upon reasonable request.

References

1. Hernandez-Estrada, E.; Lastres-Danguillecourt, O.; Robles-Ocampo, J.B.; Lopez-Lopez, A.; Sevilla-Camacho, P.Y.; Perez-Sariñana, B.Y.; Dorrego-Portela, J.R. Considerations for the Structural Analysis and Design of Wind Turbine Towers: A Review. *Renew Sust Energ Rev* **2021**, *137*, doi:10.1016/j.rser.2020.110447.
2. Zhang, C. Research on the Technology of Loads and Fatigue for Critical Components of Wind Turbine Drivetrain. Master, Zhejiang University, 2013.
3. Zhao, Z.Y.; Wu, P.H.; Xia, B.; Skitmore, M. Development Route of the Wind Power Industry in China. *Renew Sust Energ Rev* **2014**, *34*, 1-7, doi:10.1016/j.rser.2014.01.071.
4. Bartolomé, L.; Teuwen, J. Prospective Challenges in the Experimentation of the Rain Erosion on the Leading Edge of Wind Turbine Blades. *Wind Energy* **2019**, *22*, 140-151, doi:10.1002/we.2272.
5. Slot, H.M.; Gelinck, E.R.M.; Rentrop, C.; van der Heide, E. Leading Edge Erosion of Coated Wind Turbine Blades: Review of Coating Life Models. *Renew Energ* **2015**, *80*, 837-848, doi:10.1016/j.renene.2015.02.036.
6. Gui, Y. The Rain Erosion Effects on Polyurethane Coating for Wind Blade. Master, Wuhan University of Technology, 2019.
7. Verma, A.S.; Vedvik, N.P.; Haselbach, P.U.; Gao, Z.; Jiang, Z.Y. Comparison of Numerical Modelling Techniques for Impact Investigation on a Wind Turbine Blade. *Composite Structures* **2019**, *209*, 856-878, doi:10.1016/j.compstruct.2018.11.001.
8. Hu, W.F.; Chen, W.Y.; Wang, X.B.; Liu, Z.Y.; Tan, J.R.; Wang, Y.Q. Wind Turbine Blade Coating Fatigue Induced by Raindrop Impact. *Proceedings of the Asme 2020 Power Conference (Power2020)* **2020**.
9. Littell, J.D.; Ruggeri, C.R.; Goldberg, R.K.; Roberts, G.D.; Arnold, W.A.; Binienda, W.K. Measurement of Epoxy Resin Tension, Compression, and Shear Stress-Strain Curves Over a Wide Range of Strain Rates Using Small Test Specimens. *J Aerospace Eng* **2008**, *21*, 162-173, doi:10.1061/(Asce)0893-1321(2008)21:3(162).
10. Amirzadeh, B.; Louhghalam, A.; Raessi, M.; Tootkaboni, M. A Computational Framework for the Analysis of Rain-Induced Erosion in Wind Turbine Blades, Part I: Stochastic Rain Texture Model and Drop Impact Simulations. *J Wind Eng Ind Aerod* **2017**, *163*, 33-43, doi:10.1016/j.jweia.2016.12.006.
11. Best, A.C. The Size Distribution of Raindrops. *Quarterly Journal of the Royal Meteorological Society* **2010**, *76*.
12. Meteorologic Disaster Prevention and Mitigation. GB/T 28592—2012 Grade of Precipitation. Standards Press of China: Beijing, 2011.
13. Amirzadeh, B.; Louhghalam, A.; Raessi, M.; Tootkaboni, M. A Computational Framework for the Analysis of Rain-Induced Erosion in Wind Turbine Blades, Part II: Drop Impact-Induced Stresses and Blade Coating Fatigue Life. *J Wind Eng Ind Aerod* **2017**, *163*, 44-54, doi:10.1016/j.jweia.2016.12.007.

AUTHOR BIOGRAPHIES

	**Xiufeng Xu** D.Eng, Professor, Working at Mechatronic Engineering, Tongji University. Research Direction: Mechatronic Engineering. Email: xuxiufeng@tongji.edu.cn		**Yichao Xu** M.E. Studying at Mechatronic Engineering, Tongji University. Research Direction: Rain Erosion of Wind Turbine Blades. Email: 2518933281@qq.com
	**Aiguo Zhou** D.Eng, Associate Professor, Working at Mechatronic Engineering, Tongji University. Research Direction: Mechatronic Drive & Control, Robot Dynamics Modeling, Automotive Sensors, Biological Instruments. Email: zhouaiguo@tongji.edu.cn		**Zhengzhao Lai** M.E. Studying at Mechatronic Engineering, Tongji University. Research Direction: Rain Erosion of Wind Turbine Blades. Email: 2132695@tongji.edu.cn

 https://doi.org/10.59238/j.pt.2024.02.001